

# Kinetic Modulation of HERG Potassium Channels by the Volatile Anesthetic Halothane

Jichang Li, M.D., Ph.D.\* Ana M. Correa, Ph.D.†

**Background:** *HERG* (human ether-a-go-go related gene) encodes the cardiac rapidly activating delayed rectifier potassium currents ( $I_{Kr}$ ), which play an important role in cardiac action potential repolarization. General anesthetics, like halothane, can prolong Q-T interval, suggesting that they act on myocellular repolarization, possibly involving *HERG* channels. Evidence for direct modulation of *HERG* channels by halothane is still lacking. To gain insight on *HERG* channel modulation by halothane the authors recorded macroscopic currents expressed in *Xenopus* oocytes and conducted non-stationary noise analysis to evaluate single channel parameters modified by the anesthetic.

**Methods:** Macroscopic currents were recorded in 120 mM  $K^+$  internal-5 mM  $K^+$  external solutions with the cut open oocyte technique. Macropatch recordings for non-stationary noise analysis of *HERG* tail currents were made in symmetrical 120 mM  $K^+$  solutions. Pulse protocols designed for *HERG* current recording were elicited from a holding potential of -80 mV. Halothane was delivered *via* gravity-fed perfusion.

**Results:** Halothane (0.7%, 1.5%, and 3%) decreased macroscopic *HERG* currents in a concentration-dependent manner (average reduction by 14%, 22%, and 35% in the range of -40 mV to 40 mV) irrespective of potential. *HERG* currents had slower activation and accelerated deactivation and inactivation. Non-stationary noise analysis revealed that halothane, 1.5%, decreased channel  $P_o$  by 27%, whereas single-channel current amplitudes and number of channels in the patch remained unchanged.

**Conclusions:** Halothane inhibits *HERG* currents expressed in *Xenopus* oocytes in a concentration-dependent manner. It slowed down activation and accelerated deactivation and inactivation of *HERG* channels. The authors' results demonstrate that halothane decreased *HERG* currents by modulating kinetic properties of *HERG* channels, decreasing their open probability. Partial block of  $I_{Kr}$  currents could contribute to delayed myocellular repolarization and altered cardiac electrophysiology.

*HERG* (human ether-a-go-go related gene) encodes the pore-forming subunits that conduct the rapidly activating delayed rectifier  $K^+$  current ( $I_{Kr}$ ) in cardiac myocytes, which play an important role in repolarization of action potentials.<sup>1-5</sup> Modulation of *HERG* can induce long QT syndrome (LQTS), which is characterized by a prolonged Q-T interval in the electrocardiogram (ECG) and predisposes affected persons to fatal arrhythmias.<sup>6-8</sup> A variety of common clinically used medications exert cardiotoxic effects by blocking  $I_{Kr}$  and the *HERG* chan-

nel and cause an excessive prolongation of the Q-T interval, leading to an acquired form of the LQTS.<sup>9</sup>

General anesthetic agents can also influence cardiac action potentials.<sup>10-14</sup> Evidence has shown that general anesthetic agents modulate  $I_{Kr}$  currents and cause marked effects on ventricular repolarization in guinea pig and rabbit hearts.<sup>10-14</sup> In halothane-anesthetized dogs, a remarkable transient increase in mid-myocardium action potential duration was detected, which lead to a transient increase in transmural dispersion of repolarization and *torsades de pointes*.<sup>15</sup> In some patients, halothane and sevoflurane were shown to increase QT dispersion (defined as the difference between QT [max] and QT [min] in the 12-lead surface ECG, which reflects regional variations in ventricular repolarization) and QTc dispersion (QTc indicates Q-T interval corrected by heart rate), which shows that both agents can cause myocardial repolarization abnormalities.<sup>16-18</sup> These facts suggest that these agents may induce side effects through action on myocellular repolarization and that they would do so by interaction with  $I_{Kr}$  currents, which are conducted by *HERG* channels. Yet, data to support that the *HERG* channel is directly modulated by general anesthetic agents are still lacking. To understand the mechanisms involved in these general anesthetics' side effects, we studied the effects of halothane on *HERG* channels expressed in *Xenopus laevis* oocytes. We used the cut-open oocyte Vaseline gap (COVG) voltage clamp technique to address effects on macroscopic properties of *HERG* currents and the patch clamp technique to identify changes in single-channel properties using non-stationary noise analysis. We found that halothane inhibits *HERG* currents in a concentration-dependent manner primarily by differential modulation of the rates of current activation and deactivation. The observed changes in kinetic properties are the probable cause for the decreased open probability we found with mean-variance analysis.

## Materials and Methods

### Materials

Frogs (*Xenopus laevis*) were purchased from either *Xenopus* I or *Xenopus* Express. Halothane was purchased from Halocarbon Laboratories, Inc. (River Edge, NJ). All other chemicals were from Sigma (St. Louis, MO).

### HERG Channel Clones and cRNA Transcription

The cDNA for *HERG* used in this study was a generous gift by Dr. Steve Goldstein, M.D., Ph.D. (Professor, De-

\* Postgraduate Researcher, † Associate Professor.

Received from the Department of Anesthesiology, University of California, Los Angeles, The David Geffen School of Medicine, Los Angeles, California. Submitted for publication December 26, 2001. Accepted for publication June 7, 2002. Supported by grant No. GM-53781, National Institutes of Health, Bethesda, Maryland (A.M.C.), and by the Department of Anesthesiology, UCLA, Los Angeles, California. Presented in part at the annual meeting of the American Society of Anesthesiologists, New Orleans, Louisiana, October 13-17, 2001.

Address reprint requests to Dr. Correa: UCLA Department of Anesthesiology, BH-509A CHS, P.O. Box 951775, Los Angeles, California 90095-7115. Address electronic mail to: nani@ucla.edu. Individual article reprints may be purchased through the Journal Web site, www.anesthesiology.org.

partment of Pediatrics and Cellular and Molecular Physiology, Boyer Center for Molecular Medicine, Yale University, New Haven, CT). The cDNA was transcribed with the commercial SP6 mMessage mMachine kit (Ambion, Austin, TX). The integrity of the transcribed RNA was assessed in agarose gels, and the concentrations were measured spectrophotometrically.

### Oocytes

*Xenopus laevis* oocytes were isolated from frog ovaries, following conventional protocols.<sup>19</sup> Oocytes were defolliculated by collagenase treatment (collagenase type A, GIBCO BRL) in  $\text{Ca}^{2+}$ -free Ringer's solution ( $\text{Ca}^{2+}$ -free OR-2: 82.5 mM NaCl, 2.5 mM KCl, 1 mM  $\text{MgCl}_2$ , 5 mM HEPES, pH 7.0 with NaOH), followed by a progressive change to the normal frog Ringer's solution containing 1.8 mM  $\text{Ca}^{2+}$ . Defolliculated oocytes were kept in Ringer's solution (standard oocyte solution) that consisted of 100 mM NaCl, 2 mM KCl, 1 mM  $\text{MgCl}_2$ , 1.8 mM  $\text{CaCl}_2$ , 5 mM HEPES-Na, and gentamicin 50  $\mu\text{g}/\text{ml}$ , pH 7.2. RNA samples (0.1–0.2 ng/nl or 2 ng/nl) were injected into the oocytes within 24 h of isolation. The injected oocytes were used for study 3–7 days after injection. All animal procedures were approved by the Animal Research Council at the University of California, Los Angeles.

### Recording Solutions

Macroscopic currents were recorded in external solution 5 KMS (5 mM potassium methane sulfonate [KMS], 115 mM sodium methane sulfonate [NaMS], 0.5 mM  $\text{CaCl}_2$ , 1.3 mM  $\text{MgCl}_2$ , 10 mM HEPES-Na, pH 7.2) and with internal solution 120 KMS (120 mM KMS, 10 mM HEPES-K, 1 mM EGTA-K, pH 7.2). For non-stationary noise analysis, currents from macropatches were recorded with the 120 KMS solution in bath and pipette. Anesthetic solutions were prepared by vaporizing halothane into the bath solution with a clinical vaporizer (Orchard Park, NY) in an equilibrator (R.S. Weber and Associate, Westlake Village, CA) for 30 min to final concentrations of 0.7 vol% ( $0.3 \pm 0.01$  mM), 1.5 vol% ( $0.7 \pm 0.01$  mM), and 3% vol% ( $1.5 \pm 0.03$  mM), approximately equivalent to 1, 2, and 4 minimum alveolar concentration (MAC), respectively. Equilibrated solutions were collected into gas-tight syringes and delivered through Teflon tubing by a gravity-fed perfusion system. Anesthetic concentrations were determined by headspace sampling with a gas chromatograph (Hewlett-Packard HP 6890 with headspace sampler HP 7694; Hewlett-Packard, Wilmington, DE) from an aliquot of the anesthetic-containing solution withdrawn directly from the equilibration chamber.

### Electrophysiology

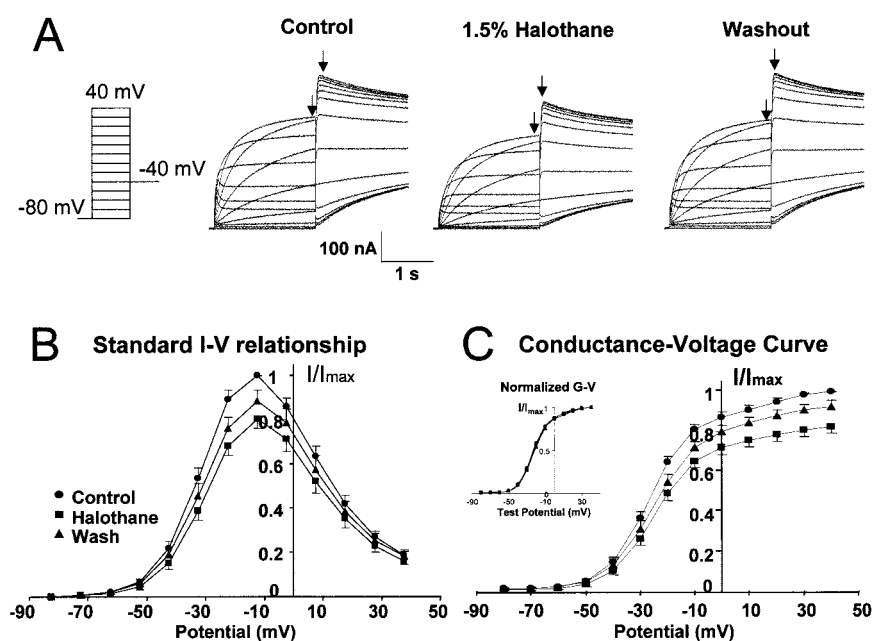
Macroscopic currents were recorded using the COVG voltage clamp technique.<sup>20</sup> The technique, described

elsewhere,<sup>20–21</sup> greatly improves the temporal resolution over that of the conventional two-electrode voltage clamp. The currents are recorded from an area of the oocyte equivalent to one-fifth to one-fourth the total surface. Custom-made software and hardware are used for acquisition and analysis of data. Electrodes filled with 3 M KCl had a resistance of 0.2–0.5 M $\Omega$  when measured in the bath solution.

For non-stationary noise analysis, macropatch currents were recorded with the patch clamp technique, using an Axopatch 200A amplifier (Axon Instruments, Inc., Union City, CA) controlled by a custom-built acquisition system. Data were acquired by sampling at 20 kHz and filtered at 10 kHz. Macroscopic currents were recorded in cell-attached patches. Patch electrodes were pulled (Micropipette Puller, Sutter Instruments Corp., Novato, CA) from 7052 capillaries (Garner Glass Co., Claremont, CA). Heat-polished pipette tips had resistance of 1.0–2.0 M $\Omega$  when filled with 120 KMS.

Mean and variance of the mean were calculated using custom-made software. For this, 150 records were used to construct the mean under each experimental condition. Leak was subtracted off-line with subtraction pulses collected throughout the run. The variance of the records with respect to the mean current was computed by pairs to compensate for time-dependent shifts in the mean.<sup>22–23</sup> The relation between mean and variance is described by the equation:  $\sigma^2 = iI - I^2/N$ , where for any given potential,  $\sigma^2$  is the variance,  $i$ , the single channel current,  $I$ , the macroscopic mean current, and  $N$ , the number of channels. Values for  $N$  and  $i$  are then estimated from the fit of the variance *versus* mean data to the equation above. Because at any given time,  $I(t) = NiP_o(t)$ , where  $P_o$  is the probability of opening, the apex of the parabola that relates the variance to the mean is at the point at which the probability of opening is 0.5; at either end,  $P_o = 0$  or  $P_o = 1$ , the variance is zero. There are two important issues that need to be mentioned. First, to get the most accurate estimates of  $N$ , the  $P_o$  should be as high as possible, the reason for which we chose to run the mean variance analysis of tail currents. Second, although not a quantitative measure, an increase in  $P_o$  can be visualized directly from the plot of the variance *versus* the mean. The limiting value of  $P_o$  shown in the tables was calculated from  $I = NiP_o$  where, in this case,  $I$  is the peak value of the mean current during the pulse, and the values of  $N$  and  $i$  were obtained from the fit of the variance–mean plot as described above. The single-channel conductance,  $\gamma_o$ , was calculated from the relation:  $i = \gamma_o(V - V_{\text{rev}})$ , where  $i$  is the single-channel current estimated from the mean-variance analysis,  $V$  is the pulse potential, and  $V_{\text{rev}}$  is the reversal potential, which in 120 mM external  $\text{K}^+$  is close to 0 mV. All experiments were conducted at room temperature (21–23°C).

Fig. 1. Halothane blocks *HERG* currents. (A) Families of currents recorded before, during, and after perfusion with 1.5% halothane following the pulse protocol shown in the inset. Currents were measured (see arrows) at the end of the depolarizing test pulses (I-V curve in B) and at the peak of the tail current at -40 mV (G-V curve in C). (B) Outward currents gave the standard I-V relationship a bell-shaped appearance (●) with  $I_{\text{peak}}$  at -10 mV. Individual I-V curves were normalized to their respective control  $I_{\text{peak}}$ . Halothane, 1.5%, (■) inhibited the currents at all potentials throughout the voltage range tested ( $n = 10$ ). (C) Peak tail currents at -40 mV (●) as a function of test pulse voltage. Halothane, 1.5%, (■) inhibited tail currents for all test voltages positive to -50 mV. Current inhibition reversed partially after wash (▲). Data are the average of 10 experiments each normalized to its respective control value at 40 mV. Curves are fits of the data to single Boltzmann functions with fitted parameters  $V_{1/2}$  and  $k$  as follow:  $V_{1/2} = -22.9 \pm 0.6$  mV and  $k = 8.9 \pm 0.5$  for the control;  $V_{1/2} = -21.8 \pm 0.5$  mV and  $k = 8.8 \pm 0.4$  for 1.5% halothane; and  $V_{1/2} = -21.2 \pm 0.4$  and  $k = 9.3 \pm 0.4$  after wash. (Inset) The normalized conductance-voltage relationship showed no apparent halothane-induced voltage shift in the conductance.



### Statistics

Data analysis was performed with Analysis (custom made) and Sigmaplot 5.0 (SPSS Inc. Jandel Scientific, San Rafael, CA) software. A nonlinear least-square curve fitting was used to perform curve-fitting procedures. Group data are expressed as mean  $\pm$  SEM. Differences between control and treatment in a group were evaluated using paired *t* test. Differences between groups were evaluated using Student *t* test. A two-tailed *P* value less than 0.05 was taken as statistically significant.

## Results

### Inhibition of *HERG* Currents by Halothane

In the oocytes injected with *HERG* mRNA, typical currents were elicited by depolarizing pulses from a holding potential of -80 mV (fig. 1A). *HERG* currents activated at potentials greater than -60 mV reached a peak at around -10 mV and then decreased at more positive potentials, giving the standard I-V relationship a typical bell-shaped appearance (fig. 1B). The tail current on going back to -40 mV (fig. 1A), after the stimulating pulse had been completed, increased with depolarizing voltages and reached a plateau value at test potentials positive to +20 mV (fig. 1C). The macroscopic current-voltage (I-V) and conductance-voltage (G-V) plots in figure 1 show the average of 10 experiments performed before, during, and after treatment with 1.5% halothane. Halothane decreased pulse and tail current amplitudes for all test potentials positive to -40 mV.

Halothane significantly decreased macroscopic *HERG* currents in a concentration-dependent manner as deter-

mined from standard current- and conductance-voltage relations (figs. 1 and 2). Figure 2A shows sample traces before and after treatment with 0.7%, 1.5%, and 3% halothane. The anesthetic induced a differential decrease in pulse and tail current amplitudes at the test pulse to -10 mV and going back to -40 mV. The maximum current at -10 mV decreased by  $10.7 \pm 4.3\%$ ,  $19.7 \pm 4.3\%$ , and  $29.4 \pm 1.3\%$  (fig. 2B), and peak tail current on repolarization to -40 mV from the depolarizing pulse to -10 mV was reduced by  $10.1 \pm 2.7\%$ ,  $19.4 \pm 3.5\%$ , and  $32.5 \pm 3.6\%$ , respectively, in the presence of 0.7%, 1.5%, and 3% halothane. This inhibitory effect is specific to halothane because perfusion with the bath solution alone had no effect on *HERG* currents, and the effects were partially reversed by washout of the drug (fig. 1). To better understand this inhibitory effect of halothane, we investigated possible voltage-dependent block of *HERG* channels by comparing the G-V curves (inset fig. 1C). When individual peak test or tail currents were normalized to the maximal control amplitude, we did not find significant changes in the shape of the I-V relationships (not shown) and did not observe a significant shift of the mid-activation fit to the G-V curves normalized to their respective peak values. Further, the fraction of peak test and tail currents inhibited by halothane did not change significantly with test voltage (figs. 2B and C). Taking the mean value for all voltages in the range of -40 mV to 40 mV, the respective average reductions in the presence of 0.7%, 1.5%, and 3% halothane were  $14.0 \pm 1.4\%$ ,  $21.7 \pm 1.9\%$ , and  $34.5 \pm 2.0\%$  as measured from peak test currents (fig.

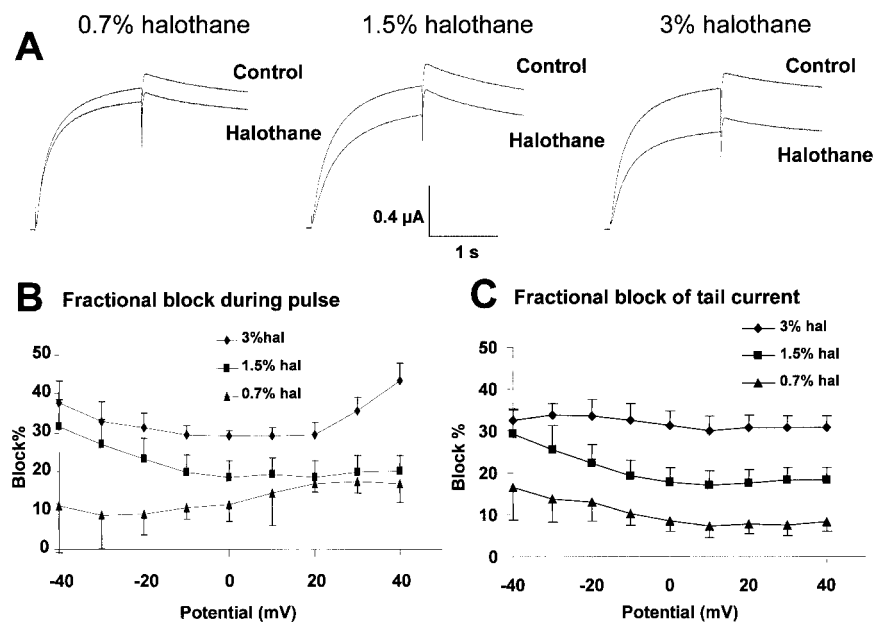


Fig. 2. Concentration dependence of current inhibition. (A) Sample data before and after 0.7%, 1.5%, and 3% halothane treatment. Currents shown were obtained pulsing to  $-10$  mV and then to  $-40$  mV. For comparison, all traces were normalized to the control at 1.5% halothane. (B) The plot shows the average current block by 0.7%, 1.5%, and 3% halothane as a function of test potential. For depolarizations between  $-40$  mV to  $+40$  mV, the average block was  $14.0 \pm 1.4\%$ ,  $21.7 \pm 1.9\%$ , and  $34.5 \pm 2.0\%$  for 0.7%, 1.5%, and 3% halothane, respectively. (C) Average tail current block at  $-40$  mV after treatment with 0.7%, 1.5%, and 3% halothane as a function of the depolarizing test potential. The average block within the range  $-40$  mV to  $40$  mV was  $10.3 \pm 1.1\%$ ,  $20.6 \pm 1.4\%$ , and  $31.7 \pm 0.4\%$  with 0.7%, 1.5%, and 3% halothane.

2B) and  $10.3 \pm 1.1\%$ ,  $20.6 \pm 1.4\%$ , and  $31.7 \pm 0.4\%$  as determined from tail currents (fig. 2C). From these results, we concluded that the drug did not exert a significant voltage-dependent block on *HERG*.

Because the effect of halothane on I-V and G-V curves, measured as shown in figure 1A, was determined while inactivation of the channel had already developed, we investigated if halothane exerted its effect by specific action on the inactivated state by studying the blocking effect of halothane after removal of inactivation. The protocol used is depicted in the inset of figure 3A in which a 2-s prepulse to  $20$  mV (used to open the chan-

nels) was followed by a short 15-ms pulse to  $-120$  mV (a pulse long enough for rapid recovery from inactivation, but short enough to prevent significant deactivation), after which, a family of test pulses to the potentials ranging from  $-150$  mV to  $20$  mV was applied (fig. 3). Figure 3A shows families of curves before and after halothane obtained in this manner. Halothane exerted its inhibitory effect along all the voltage range from  $-150$  to  $20$  mV, with an average block of  $14.0 \pm 0.8\%$ ,  $25.3 \pm 0.4\%$ , and  $37.4 \pm 0.4\%$ , respectively, in 0.7%, 1.5%, and 3% halothane ( $P < 0.05$ , fig. 3). The results indicated that halothane could exert its effect in the absence of inactivation.

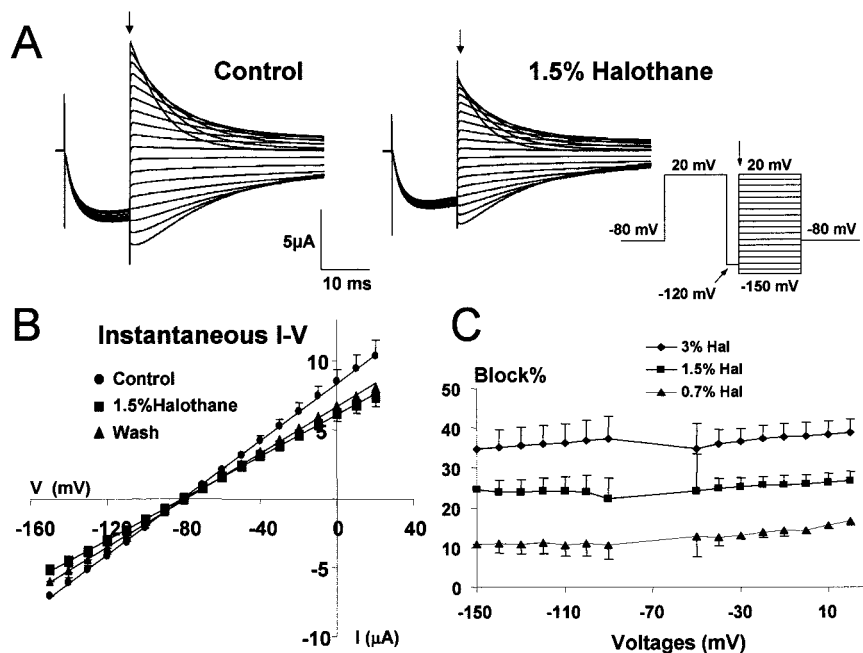
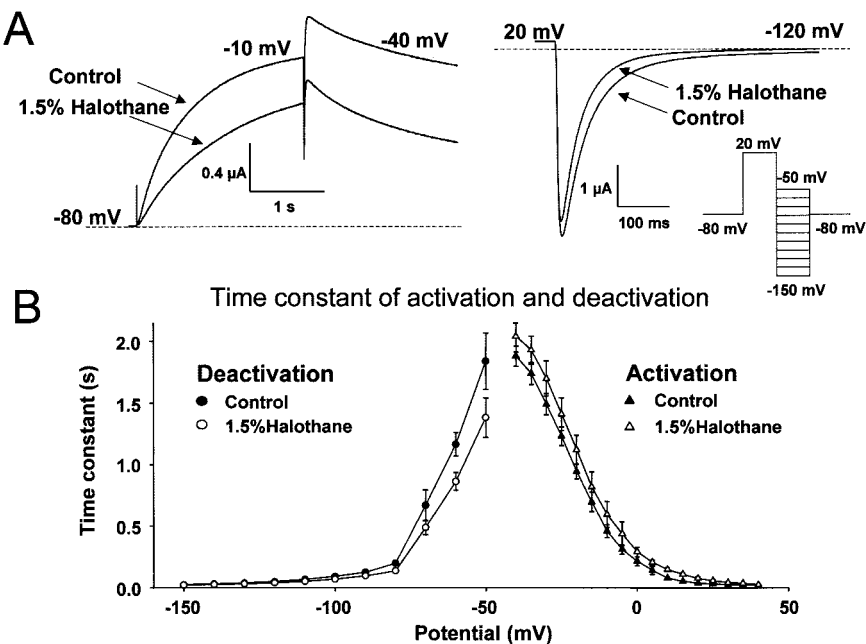


Fig. 3. Effect of halothane on *HERG* channel instantaneous I-V relationship. (A) Sample currents, control, and after treatment with 1.5% halothane, obtained with the pulse protocol shown in the inset. (B) Instantaneous I-V relationship built from current amplitude measured at the beginning of the test depolarization (arrows in A). The I-V relation was linear in the control ( $\bullet$ ), after perfusion of halothane ( $\blacksquare$ ), and after wash ( $\blacktriangle$ ). Halothane induced a significant ( $P < 0.01$ ), partially reversible depression of *HERG* currents. (C) The plot shows the % block by 0.7%, 1.5%, and 3% halothane as a function of test potential. Halothane, 0.7%, 1.5% and 3%, induced an average block of  $12.9 \pm 0.3\%$ ,  $24.9 \pm 0.4\%$ , and  $36.8 \pm 0.4\%$  between  $-150$  mV and  $20$  mV. Points in the vicinity of current reversal were not plotted.

**Fig. 4.** Halothane changed *HERG* current activation and deactivation rates. **(A)** Left, sample traces of currents at  $-10$  mV elicited following the I-V protocol shown in figure 1A, inset. Right, sample traces of currents at  $-120$  mV after a test pulse to  $20$  mV obtained following the protocol shown in the inset. Control and 1.5% halothane records are shown superimposed; the halothane trace was scaled to match the control current value at  $20$  mV. Dashed lines represent the zero current level. **(B)** Activation and deactivation time constants as a function of voltage. Activation time course was fit to a single exponential relaxation. Double exponential relaxation was used to fit deactivation time courses. *HERG* currents after 1.5% halothane treatment had slower activation (control *vs.* 1.5% halothane:  $459 \pm 52$  ms *vs.*  $595 \pm 105$  ms at  $-10$  mV, and  $76 \pm 11$  ms *vs.*  $147 \pm 38$  ms at  $10$  mV,  $n = 5$ ), and accelerated deactivation (control *vs.* halothane:  $49.4 \pm 1.4$  ms *vs.*  $39.4 \pm 1.7$  ms at  $-120$  mV, and  $91.8 \pm 4.0$  ms *vs.*  $69.8 \pm 3.9$  ms at  $-100$  mV,  $n = 5$ ). Differences were significant between  $-10$  mV and  $40$  mV for activation and in the range between  $-150$  mV and  $-50$  mV for deactivation.



### Modification of *HERG* Channel Kinetics

To further characterize and understand the inhibitory effect of halothane on *HERG* channels, we specifically investigated changes in channel kinetics induced by the anesthetic. First, we studied effects on channel activation. The time course of current activation was fit to a single exponential relaxation for test potentials in the range of  $-50$  mV to  $40$  mV. Halothane decreased the rate of activation of *HERG* currents (fig. 4). Relative to the control, *HERG* currents after halothane treatment activated more slowly with time constants increased by  $12.7 \pm 10.7\%$ ,  $28.5 \pm 11.4\%$ , and  $35.1 \pm 9.9\%$  at  $-10$  mV, and by  $23.4 \pm 13.0\%$ ,  $100.4 \pm 20.4\%$ , and  $167.8 \pm 15.4\%$  at  $10$  mV during perfusion of 0.7%, 1.5%, and 3% halothane, respectively (see also table 1). To determine the time constant of current deactivation, a 2-s pre-depolarizing pulse to  $20$  mV was used to fully open the channels; a family of test potentials then was given, and tail current decay was fitted to double exponential functions at potentials ranging from  $-50$  mV to  $-150$  mV. Halothane significantly altered the

deactivation rate of the tail current, accelerating the fast component of current deactivation. Time constants decreased by  $14.7 \pm 3.6\%$ ,  $20.2 \pm 2.7\%$ , and  $26.2 \pm 5.0\%$  at  $-120$  mV with perfusion of 0.7%, 1.5%, and 3% halothane, respectively (table 1). Differences were significant between  $-10$  mV and  $40$  mV for activation ( $P < 0.05$ ) and in the range of  $-150$  mV and  $-80$  mV for deactivation ( $P < 0.05$ ). Both changes would produce an apparent reduction in current amplitude.

In addition, we also observed changes in the onset of inactivation during perfusion of halothane. The oocytes were first depolarized to  $20$  mV for 2 s to inactivate the channels, and after a brief 15-ms repolarizing pulse to  $-120$  mV to induce rapid recovery from inactivation without introducing significant deactivation, a train of test pulses from  $-150$  mV to  $60$  mV was given to force the channels previously inactivated to reactivate. The time course of the current decay during the more positive test pulses, therefore, represents the onset of inactivation. We tested for the effects of halothane on the

**Table 1.** Time Constant of Activation and Deactivation

Potentials		Time Constant of Activation (ms)					Fast Component of Time Constant of Deactivation (ms)			
		-40 mV	-20 mV	0 mV	20 mV	40 mV	-140 mV	-120 mV	-100 mV	-80 mV
0.7% (n = 5)	Control	1,332.3 ± 109.5	495.9 ± 75.9	91.7 ± 16.5	29.2 ± 3.5	17.2 ± 2.0	25.7 ± 1.8	43.3 ± 2.7	87.9 ± 7.2	192.3 ± 13.8
	Halothane	1,373.1 ± 129.5	498.0 ± 55.8	115.5 ± 17.1*	39.5 ± 9.0	31.2 ± 7.5	22.4 ± 2.1*	37.1 ± 3.4*	73.1 ± 8.6*	155.7 ± 16.6*
1.5% (n = 10)	Control	1,878.7 ± 81.7	944.0 ± 60.1	213.8 ± 35.3	36.0 ± 3.1	20.0 ± 1.0	31.0 ± 0.6	49.4 ± 1.4	91.8 ± 4.0	199.6 ± 18.6
	Halothane	2,044.9 ± 124.7	1,121.3 ± 118.1	290.9 ± 38.5*	75.8 ± 12.1*	24.1 ± 3.9*	25.9 ± 1.1*	39.4 ± 1.7†	69.8 ± 3.9†	137.5 ± 10.7*
3% (n = 7)	Control	1,362.2 ± 111.9	634.9 ± 120.0	167.3 ± 49.3	37.4 ± 7.5	14.4 ± 2.5	30.8 ± 2.3	53.4 ± 4.3	107.7 ± 9.2	225.8 ± 17.0
	Halothane	1,623.8 ± 208.1*	819.2 ± 169.4*	293.7 ± 70.6*	100.0 ± 23.2*	32.1 ± 9.3*	23.3 ± 1.9*	39.0 ± 3.4*	77.3 ± 8.1†	150.4 ± 13.1*

\*  $P < 0.05$  and †  $P < 0.01$  versus control.

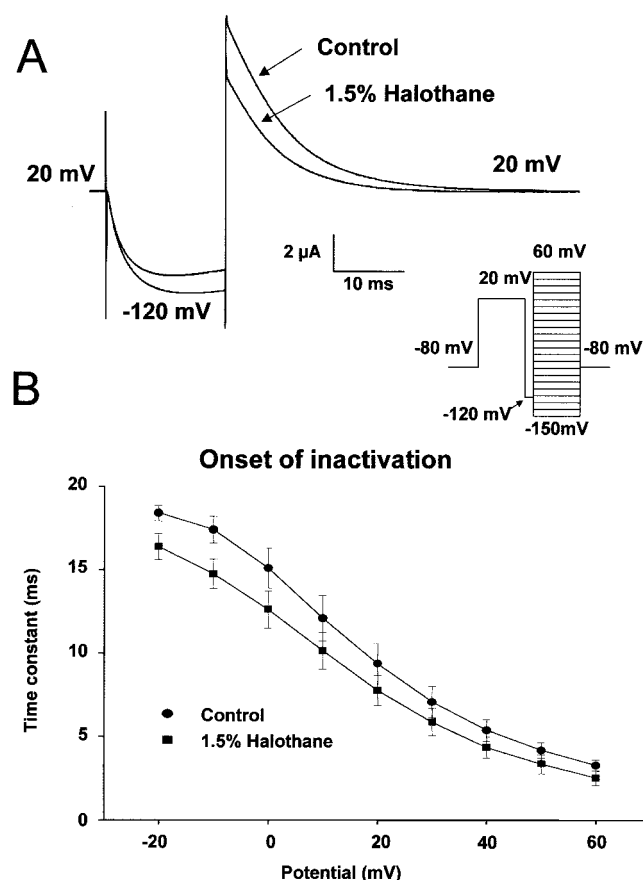


Fig. 5. Halothane accelerated the rate of inactivation. (A) To study onset of inactivation, the pulse protocol shown in the inset was followed. The superimposed traces (left) illustrate the difference between control and anesthetic-treated currents for a test pulse to 20 mV. The initial decay of the currents after the pulse to  $-120$  mV described the onset of inactivation. (B) Time constants obtained from a single exponential fit to the decay of the current expressed as a function of voltage. Halothane accelerated the rate of channel inactivation at all potentials. The differences were significant to  $P < 0.05$ .

onset of inactivation by fitting these currents to a single exponential decay. We found that halothane also could accelerate the calculated macroscopic time constants for the onset of inactivation for all test potentials. The differences were significant to  $P$  less than 0.05 (see data in fig. 5 and table 2).

### Changes in Steady-state Inactivation of HERG Channels

The steady-state inactivation of the channels was studied using a double-pulse protocol with varying interpulse potential amplitude. First, a prepulse to 20 mV for 2 s was used to fully activate and inactivate the channels, followed by a brief 15-ms interpulse, ranging from  $-120$  mV to 60 mV (this brief pulse was long enough for rapid recovery from inactivation, but short enough to prevent significant deactivation or for significant additional inactivation, depending on the step potential), and finally followed by a test pulse to 20 mV. Currents were measured immediately after the 15-ms pulses. As previously mentioned, the maximal amplitude of the current during the test pulse to 20 mV represents the number of channels not inactivated during the interpulse. To obtain a reliable measure of the maximal current, we extrapolated each single exponential fit of the currents to the end of the repolarizing interpulse. This procedure enabled us to minimize the contribution of the capacitive current to our measurements. The voltage dependence of steady-state inactivation was operationally defined as the amplitude of the extrapolated peak current against the interpulse potential (fig. 6). We could see that halothane, wash, and control data superimpose for most of the voltage range up to  $-60$  mV. At potentials negative to  $-60$  mV, currents in halothane were clearly smaller relative to the control, and the currents at  $-120$  mV were  $81.8 \pm 2.3\%$ ,  $74.9 \pm 3.4\%$ , and  $60.3 \pm 3.1\%$  of control with 0.7%, 1.5%, and 3% halothane. This would indicate that fewer channels recover from inactivation in the presence of the anesthetic agent. Alternatively, it could be a consequence of faster deactivation kinetics as shown in figure 4.

### Nonstationary Noise Analysis of Macroscopic Tail Currents

Noise analysis is a powerful tool to investigate single-channel properties from macroscopic current recordings because it yields reliable quantitative estimates of single-channel parameters.<sup>23</sup> For a homogeneous population of statistically independent channels, the mean current,  $I(t)$ , and the current variance,  $\sigma_I(t)^2$ , are given

Table 2. Time Constant of Inactivation

Potentials		Time Constant of Inactivation (ms)				
		$-20$ mV	$0$ mV	$20$ mV	$40$ mV	$60$ mV
0.7% (n = 5)	Control	$19.2 \pm 0.9$	$13.7 \pm 1.5$	$7.9 \pm 1.5$	$4.4 \pm 1.1$	$2.7 \pm 0.8$
	Halothane	$18.9 \pm 0.7$	$12.9 \pm 1.3$	$7.0 \pm 1.3$	$3.9 \pm 1.0$	$2.4 \pm 0.8$
1.5% (n = 5)	Control	$18.6 \pm 0.5$	$15.4 \pm 1.3$	$9.8 \pm 1.3$	$5.6 \pm 0.7$	$3.4 \pm 0.4$
	Halothane	$17.0 \pm 0.5^*$	$13.4 \pm 1.0^*$	$8.3 \pm 0.9^*$	$4.7 \pm 0.6^*$	$2.8 \pm 0.4^*$
3% (n = 5)	Control	$21.7 \pm 1.4$	$15.6 \pm 1.2$	$8.9 \pm 0.8$	$5.0 \pm 0.5$	$3.0 \pm 0.3$
	Halothane	$19.7 \pm 1.0^*$	$13.8 \pm 0.9^\dagger$	$7.7 \pm 0.6^*$	$4.1 \pm 0.3^*$	$2.3 \pm 0.2^*$

\*  $P < 0.05$  and  $^\dagger P < 0.01$  versus control.

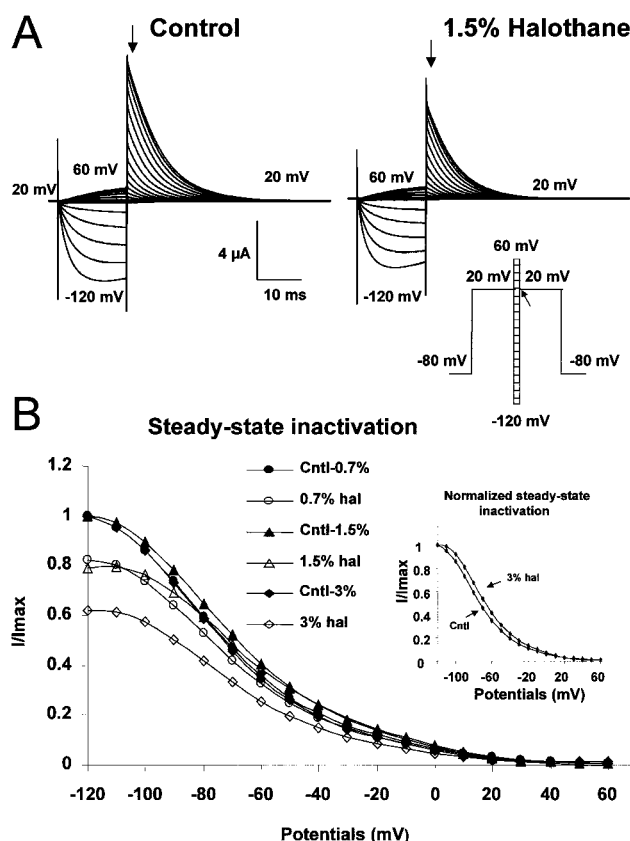


Fig. 6. Effect of halothane on the steady-state inactivation. (A) Sample control and 1.5% halothane experimental traces recorded following the pulse protocol shown in the inset. Currents were measured immediately after the 15-ms test pulses (arrow). (B) The steady-state inactivation curves before and after perfusion with 0.7%, 1.5%, and 3% halothane are shown for the average of five experiments. Control and halothane data superimpose for the voltages positive to  $-10$  mV. At more negative potentials, currents in halothane were clearly smaller relative to the control. (Inset) Sample normalized steady-state inactivation curves before (diamonds) and after (open diamonds) 3% halothane. After halothane treatment, inactivation curves were right-shifted by 4–8 mV, but the difference was not significant for all halothane concentrations tested.

by the following equations:  $I(t) = NiP_o(t)$  and  $\sigma_I^2(t) = Ni^2 P_o(t)[1 - P_o(t)]$ . Provided that  $I$  and  $\sigma^2$  are estimated from various open probabilities ( $P_o$ ),  $i$  (the single-channel current amplitude) and  $N$  (the number of channels) can be determined by fitting mean-variance data according to  $\sigma^2 = iI - I^2/N$ . During a depolarization, *HERG* channels inactivate much faster than they activate, and the currents of the fully open channels during depolarizing pulses usually cannot be recorded. A better estimate of the currents can be obtained on quick repolarization after depolarizing pulses because recovery from inactivation is much faster than deactivation of the channels. Considering these specific properties of *HERG* channels, we analyzed the non-stationary noise of tail currents. We used double-pulse protocols to perform the tail current noise analysis, *i.e.*, a 1-s depolarizing pulse to 40 mV was given to fully open (and inactivate) the

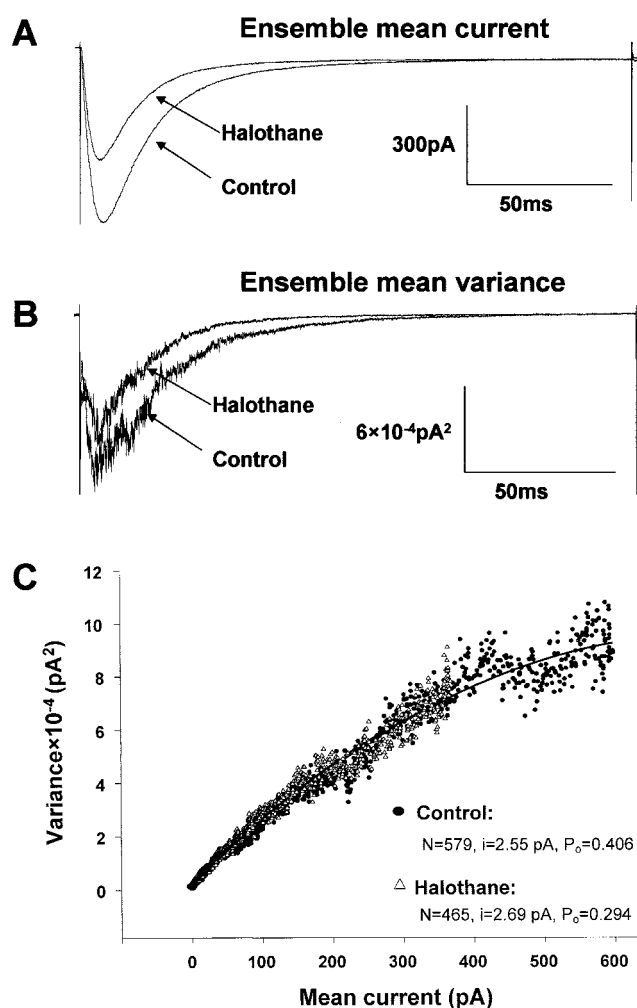


Fig. 7. Non-stationary noise analysis of macroscopic tail currents is shown. (A) Averaged tail currents recorded from macro-patches in response to a repolarization to  $-140$  mV after completion of a 1-s positive pulse to 40 mV. The traces are averages of 150 records before (control) and after perfusion of 1.5% halothane to the bath (halothane), which resulted in an approximate decrease in current of 38.5% measured at the peak of the tail current. (B) Averaged ensemble variance of the experiment shown in A. Variance computed by pairs.<sup>24</sup> (C) Sample variance as a function of mean current. The continuous curves represent data fits to the equation  $\sigma^2 = iI - I^2/N$  (Materials and Methods section). The fits yielded the indicated values for the single-channel current and number of channels. Data were filtered at 10 kHz. Pipette: 120 KMS; bath: 120 KMS.

channels, and then a test pulse to  $-140$  mV was generated to induce tail currents. Consistent with the data obtained from COVG recordings, 1.5% halothane significantly decreased the tail currents by an average of 27.7% and accelerated the fast component of deactivation by 13%. Figure 7 provides an example of non-stationary noise analysis of macroscopic tail currents. In this experiment, 1.5% halothane did not significantly affect the amplitude of single-channel event or the number of channels in the patch, whereas the maximum open probabilities, obtained from the equation  $I = NiP_o$ , decreased significantly by 27.6% (0.406 *vs.* 0.294; patch 1,

Table 3. Single Channel Parameters from Noise Analysis of Tail Currents

	Patch No.					Mean $\pm$ SEM	P (< 0.05)	$\Delta\%$
	1	2	3	4	5			
Control								
I (pA)	598.5	1,133.5	917.1	841.7	1,089.1	916.0 $\pm$ 95.8	—	—
i (pA)	2.55	1.89	2.14	2.10	2.36	2.21 $\pm$ 0.11	—	—
P <sub>o</sub>	0.406	0.319	0.41	0.306	0.596	0.407 $\pm$ 0.052	—	—
$\gamma_o$ (pS)	18.2	13.5	15.3	15.0	16.9	15.8 $\pm$ 0.8	—	—
N	579	1,879	1,037	1,311	774	1,116 $\pm$ 227	—	—
Halothane								
I (pA)	368.2	1,011.1	540.9	704.2	741.7	673.2 $\pm$ 107.3	0.0097	-27.7 $\pm$ 6.0
i (pA)	2.69	1.85	2.23	1.89	1.93	2.11 $\pm$ 0.16	0.4371	-4.2 $\pm$ 4.5
P <sub>o</sub>	0.294	0.271	0.250	0.257	0.384	0.291 $\pm$ 0.024	0.0218	-26.6 $\pm$ 4.9
$\gamma_o$ (pS)	19.2	13.2	15.9	13.5	13.8	15.1 $\pm$ 1.1	0.4263	-4.2 $\pm$ 4.5
N	465	2,016	969	1,448	1,001	1,180 $\pm$ 261	0.3865	4.2 $\pm$ 8.3

I = mean macroscopic tail current; i = the single channel current; P<sub>o</sub> = maximum open probability, calculated according to  $I = N \cdot P_o \cdot i$ ;  $\gamma_o$  = single channel conductance, calculated according to  $i = \gamma_o \cdot (E - E_{rev})$ , where E is the pulse potential, and E<sub>rev</sub> is the reversal potential; N = number of channels.

table 3). The results from five such experiments are given in table 3. On average, the calculated values of P<sub>o</sub> were significantly smaller in halothane (control *vs.* halothane: 0.407  $\pm$  0.052 *vs.* 0.291  $\pm$  0.024, respectively;  $P < 0.05$ ), whereas changes in *i* and N were not significant (table 3) and were also less consistent. The single-channel conductance,  $\gamma_o$ , calculated from the fitted values of *i* was 15.8  $\pm$  0.8 pS (table 3). These results further support the data obtained from cut-open oocyte recordings, that halothane accelerates inactivation and deactivation of the channels, which would lead to a decreased open probability of single-channel events.

## Discussion

*HERG* subunits coassemble to form channels that conduct a delayed rectifier K<sup>+</sup> current (I<sub>Kr</sub>) important for repolarization of cardiac myocytes.<sup>1-5</sup> Several lines of evidence suggest that volatile anesthetic agents may induce abnormalities in cardiac repolarization.<sup>10-18</sup> Because I<sub>Kr</sub> is a principal repolarizing current in cardiac myocytes and little is known how general anesthetic agents affect I<sub>Kr</sub> currents, we used *HERG* as a cloned I<sub>Kr</sub> channel to explore actual effects of halothane on this channel in the virtual absence of other contaminating currents. In the present study, we demonstrated that different concentrations of halothane (0.7%, 1.5%, and 3%) significantly reduced the conductance of *HERG* channels expressed in *Xenopus* oocytes. The kinetic analysis revealed that halothane decreased current activation rate constants and increased current deactivation and inactivation rate constants in the same concentration-dependent manner, consequently causing smaller macroscopic currents. A finding of this work is that coexpression of no other subunits is required to observe halothane effects on *HERG* currents.

A decreased macroscopic conductance can result from a decrease in the single-channel conductance,  $\gamma_o$ , in the

number of channels in a patch, N, or the probability of opening, P<sub>o</sub>. The results presented in this article (fig. 7 and table 3), obtained with non-stationary noise analysis, showed that halothane did not induce significant changes in the single-channel current amplitude nor in the number of channels present in the patches. In contrast, halothane induced a significant decrease in the P<sub>o</sub> of the channels. Consistent with previously reported values of *HERG* average P<sub>o</sub>,<sup>24</sup> our results also indicated that the *HERG* channel exhibits a low P<sub>o</sub>, usually less than 0.5. To obtain reliable data from the mean-variance analysis, we designed conditions to optimize the probability of opening. Under these conditions, the P<sub>o</sub> was greatly increased to values closer to 0.5 (the apex of the parabola), but even under optimal conditions, the mean peak probability of opening of *HERG* channels was low (0.41  $\pm$  0.05). This is, in part, the result of contamination by incomplete recovery from inactivation and developing deactivation while the channels transit from the high P<sub>o</sub> state at 40 mV to the low P<sub>o</sub> state at -140 mV. Thus, in the presence of inactivation, the maximum P<sub>o</sub> will be underestimated. Using single-channel data from *HERG* channels expressed in *Xenopus* oocytes, Zhou *et al.*<sup>24</sup> reported average probabilities of 0.011 at 40 mV and of 0.17 for the first 600 ms on return to -90 mV. The average probabilities, which are determined over time, are expected to be lower than that reported here for the limiting P<sub>o</sub> at -140 mV because of the respective contribution of inactivation during the pulse to 40 mV and of recovery from inactivation and deactivation on repolarization to -90 mV. Regardless, the result that halothane further reduces the P<sub>o</sub> is consistent with an acceleration of channel deactivation.

As mentioned above, the single-channel current was not greatly affected by 1.5% halothane, and, hence, the calculated single-channel conductance,  $\gamma_o$ , was unchanged by the anesthetic agent. The control value of  $\gamma_o$  obtained here was 30% higher (15.8 pS *vs.* 12.1 pS) than

that reported previously by Zhou *et al.*<sup>24</sup> for the *HERG* channel in the same external potassium concentration. Because the  $\gamma_o$  reported in this article was calculated from the average fitted single-channel current obtained for a single voltage value at an extreme negative potential (−140 mV), it is not surprising that there would be a discrepancy; nonetheless, the values are within the same order of magnitude.

The findings with mean-variance analysis along with the observations from macroscopic recordings support the idea that the main effect of halothane is to modulate the kinetic properties of *HERG* channels in the direction of reduced overall macroscopic conductance. The marked acceleration of deactivation and inactivation in halothane hinted at an open state relatively more unstable in halothane-treated channels, which agrees well with a reduced open probability. Thus, single-channel events could exhibit faster transitions from open to inactivated state during depolarization or from open to close states during deactivation, leading to a markedly decreased open probability of the channels. A prediction resulting from this pattern of behavior is that in halothane, the mean open time of the channels would be briefer relative to controls. A reduced  $P_o$  could result from longer close times or increased flicker from the open state. Discrimination between these alternatives would have to be assessed from the analysis of single-channel data.

The concentrations of halothane used in this study, 0.7, 1.5, and 3 vol%, are close to 1, 2, and 4 MAC for halothane. At all concentrations, we found a decreased conductance and altered current kinetics, particularly at high concentrations (2 and 4 MAC). Although the effects described here, which are at concentrations equal to 1 MAC or more, are likely to occur during general anesthesia, most clinically used concentrations of halothane are held close to 1 MAC. At this concentration, the effect of halothane is rather small relative to that observed in 2 or 4 MAC; however, the effect would become more or less significant if concomitantly other depolarizing and repolarizing currents are affected by the anesthetic agent. Sodium and calcium currents, respectively the main depolarizing currents for the initiation of the action potential and during the plateau phase of the cardiac action potential, are depressed by halothane,<sup>25–27</sup> so it is not unlikely that at 1 MAC or less, the effects of halothane on  $I_{Kr}$  could be masked by an overall reduced cellular depolarization. Conversely, because  $I_{Kr}$  is not the only current to be affected by the anesthetic, even small effects may contribute to the overall loss of rhythmic function. In addition, if the many factors that influence cardiac function in clinical conditions are considered, the risk for repolarization abnormalities increases when factors that decrease potassium flux act concurrently to impair the ability of the myocardium to repolarize. Well-recognized conditions that diminish “repolarization reserve” include female gender, hypokalemia, and drugs

that inhibit cardiac potassium channels. So in these cases, clinically relevant doses or even low doses could further damage the repolarization of myocardium.

## Conclusion

Taken together, our results demonstrate that the volatile anesthetic halothane could inhibit *HERG* currents in a concentration-dependent manner and that it appeared to modulate kinetic properties of the *HERG* channel, *i.e.*, slowing activation and accelerating deactivation and inactivation of *HERG* channels. Non-stationary noise analysis indicated that halothane decreased the macroscopic conductance by decreasing the open probability of the channels. These results suggest that inhibition of *HERG* currents may contribute to an altered cardiac electrophysiology in some patients during halothane anesthesia.

The authors thank Dr. Steve Goldstein, M.D., Ph.D. (Professor of Department of Pediatrics and Cellular and Molecular Physiology, Boyer Center for Molecular Medicine, Yale University, New Haven, Connecticut) for the cDNA of the *HERG* K<sup>+</sup> channel; Dr. Francisco Bezanilla, Ph.D. (Hagiwara Professor of Neuroscience, Department of Physiology, UCLA, Los Angeles, California) for review and helpful discussion of the manuscript; Ms. Evgenia Grigorova, M.S. (Laboratory Assistant II, Department of Physiology, UCLA, Los Angeles, California) for oocyte isolation; and Mr. Ricardo Esquatin, B.S. (Staff Research Assistant, Department of Anesthesiology, UCLA, Los Angeles, California) for technical assistance.

## References

1. Trudeau MC, Warmke JW, Ganetzky B, Robertson GA: *HERG*, a human inward rectifier in the voltage-gated potassium channel family. *Science* 1995; 269:92–5
2. Curran ME, Splawski I, Timothy KW, Vincent GM, Green ED, Keating MT: A molecular basis for cardiac arrhythmia: *HERG* mutations cause long QT syndrome. *Cell* 1995; 80:795–803
3. Barry DM, Nerbonne JM: Myocardial potassium channels: Electrophysiological and molecular diversity. *Annu Rev Physiol* 1996; 58:363–94
4. Snyders DJ: Structure and function of cardiac potassium channels. *Cardiovasc Res* 1999; 42:377–90
5. Sanguinetti MC, Zou A: Molecular physiology of cardiac delayed rectifier K<sup>+</sup> channels. *Heart Vessels* 1997; (suppl 12):170–2
6. Sanguinetti MC, Jiang C, Curran ME, Keating MT: A mechanistic link between an inherited and an acquired cardiac arrhythmia: *HERG* encodes the  $I_{Kr}$  potassium channel. *Cell* 1995; 81:299–307
7. Priori AG, Napolitano C, Paganini V, Cantù F, Schwartz P: Molecular biology of the long QT syndrome: Impact on management. *PACE* 1997; 20:2052–7
8. Zhou Z, Gong Q, Epstein ML, January CT: *HERG* channel dysfunction in human long QT syndrome. *J Biol Chem* 1998; 273:21061–6
9. Vincent GM: Ventricular arrhythmias-Long QT syndrome. *Cardiol Clin* 2000; 18:309–25
10. Hirota K, Ito Y, Masuda A, Momose Y: Effects of halothane on membrane ionic currents in guinea pig atrial and ventricular myocytes. *Acta Anaesthesiol Scand* 1989; 33:239–44
11. Baum VC: Distinctive effects of three intravenous anesthetics on the inward rectifier ( $I_{Kr}$ ) and the delayed rectifier ( $I_{K}$ ) potassium currents in myocardium: implications for the mechanism of action. *Anesth Analg* 1993; 76(1):18–23
12. Park WK, Pancrazio JJ, Suh CK, Lynch C 3rd: Myocardial depressant effects of sevoflurane. Mechanical and electrophysiologic actions *in vitro*. *ANESTHESIOLOGY* 1996; 84:1166–76
13. Martynyuk AE, Morey TE, Raatikainen MJ, Seybert CB, Dennis DM: Ionic mechanisms mediating the differential effects of methohexital and thiopental on action potential duration in guinea pig and rabbit isolated ventricular myocytes. *ANESTHESIOLOGY* 1999; 90:156–64
14. Morey TE, Martynyuk AE, Napolitano CA, Raatikainen MJ, Guyton TS, Dennis DM: Ionic basis of the differential effects of intravenous anesthetics on erythromycin-induced prolongation of ventricular repolarization in the guinea pig heart. *ANESTHESIOLOGY* 1997; 87(5):1172–81
15. Weissenburger J, Nesterenko VV, Antzelevitch C: Transmural heterogeneity of ventricular repolarization under baseline and long QT conditions in the

canine heart in vivo: Torsades de pointes develops with halothane but not pentobarbital anesthesia. *J Cardiovasc Electrophysiol* 2000; 11:290-304

16. Güler N, Bilge M, Eryonucu B, Kati I, Demirel CB: The effects of halothane and sevoflurane on QT dispersion. *Acta Cardiol* 1999; 54:311-5

17. Schmeling WT, Warltier DC, McDonald DJ, Madsen KE, Atlee JL, Kampine JP: Prolongation of the QT interval by enflurane, isoflurane, and halothane in humans. *Anesth Analg* 1991; 72:137-44

18. Michaloudis D, Fraidakis O, Lefaki T, Dede I, Kanakoudes F, Askitopoulou H, Pollard BJ: Anaesthesia and the QT Interval in Humans: The Effects of Isoflurane and Halothane. *Anaesthesia* 1996; 51:219-24

19. Goldin AL: Maintenance of *Xenopus laevis* and Oocyte Injection. *Methods Enzymol* 1992; 207:266-79

20. Stefani E, Bezanilla F: The cut open oocyte voltage clamp technique. *Methods Enzymol* 1998; 293:300-18

21. Kaneko S, Akaike A, Satoh M: Cut-open recording techniques. *Methods Enzymol* 1998; 293:319-31

22. Sigg D, Stefani E, Bezanilla F: Gating current noise produced by elementary transitions in Shaker potassium channels. *Science* 1994; 264:578-82

23. Sigworth FJ: The variance of sodium current fluctuations at the node of Ranvier. *J Physiol* 1980; 307:97-129

24. Zou A, Curran ME, Keating MT, Sanguinetti MC: Single HERG delayed rectifier K<sup>+</sup> channels expressed in *Xenopus* oocytes. *Am J Physiol Heart Circ Physiol* 1997; 272:H1309-14

25. Pancrazio JJ: Halothane and isoflurane preferentially depress a slowly inactivating component of Ca<sup>2+</sup> channel current in guinea-pig myocytes. *J Physiol* 1996; 494:91-103

26. Weigt HU, Kwok WM, Rehmer GC, Bosnjak ZJ: Modulation of the cardiac sodium current by inhalational anesthetics in the absence and presence of  $\beta$ -stimulation. *ANESTHESIOLOGY* 1998; 88:114-24

27. Eskinder H, Supan FD, Turner LA, Kampine JP, Bosnjak ZJ: The effects of halothane and isoflurane on slowly inactivating sodium current in canine cardiac purkinje cells. *Anesth Analg* 1993; 77:32-7